

Research Article

Tahir Cetin Akinci*, Serhat Seker, Erkan Dursun, and Osman Kilic

Noise identification based on spectral analysis and noisy transfer function approach for fuel cells

<https://doi.org/10.1515/noise-2020-0002>

Received Nov 23, 2019; accepted Feb 25, 2020

Abstract: In this study, some measurements like the current, voltage and hydrogen flow based on the fuel cell are investigated in spectral-domain as well as their time-domain representations and then, their spectral properties are extracted. Besides this, taking the simplified transfer function approach into account, which is defined between the hydrogen flow and current of the cell as an input-output pair, more detailed results are obtained. Therefore, the spectral parts of the fuel cell are put into categories under the impacts coming from the process, measurement circuits and digitizers. The process noise to be defined at very small frequencies (<15 Hz) can be explained as the effects of the various physical and chemical interactions emerging in the fuel cell. Moreover, this study analysed the spectral characteristics of fuel cells for current, voltage and hydrogen flow in detail.

Keywords: hydrogen energy, fuel cell, time-frequency analysis, spectral analysis, transfer function, noise

1 Introduction

Fuel cells are predicated on electrochemical energy conversion which is a direct conversion from the chemical energy of the fuel to DC electricity [3]. In this manner, we can operationally describe fuel cells as a DC source [2, 5, 8, 11]. In many applications, like automotive, the fuel type is hydrogen [7, 13]. Here, the basic electrochemical reaction is represented by the combination of the hydrogen and oxygen

[4, 10, 12, 22]. According to this description, the fuel cell generates DC electricity, waste heat and water. Its use in technological applications is quite significant even though it is based on a very simple electrochemical reaction. One of the most important aspects of energy conversion is efficiency and the cost of generated energy. Today, the fuel cells are a very promising energy technology when they are compared with the existing, conventional energy conversion technologies. Their superiorities over the conventional ones can be listed as:

- High efficiency
- Very low or zero emissions
- Simplicity and low cost
- No moving parts and relatively long life
- Modular structure, Size and weight
- Quiet

In this manner, fuel cells are compact, economical and very reliable sources to provide clean energy [14].

A Polymer Electrolyte Membrane (PEM) fuel cell consists of flow collectors, water management subsystem, an anode and a cathode, which is separated by a very thin membrane. Hydrogen and oxygen gases are respectively catered to anode and cathode sides through gas flow channels. Hydrogen molecules are oxidized at the anode to protons and electrons. Here, the protons pass through the membrane while the electrons are transferred to the cathode by an external circuit system. Following this process, the protons and electrons are combined with supplied oxygen to form water as waste [6, 15, 16, 24].

Performance of the PEM fuel cell systems is correlated with the local water content in the membrane [1, 17]. High humidity leads to the rise in fuel cell efficiency, and thus, it precludes cell degradation [9, 20]. Whereas, excessive damp causes condensed droplets in the flow channels, and then, it can block the reaction [21]. Also, water formed at the cathode must quickly leave the cathode to allow oxygen to reach the cathode catalyst layer. Without sufficient humidification of the membranes, the proton conduction will not work. To design more stable and efficient systems, it is desired to identify water content changes during the operation of the fuel cell [15, 18].

*Corresponding Author: **Tahir Cetin Akinci:** Department of Electrical Engineering, Istanbul Technical University, Maslak, Istanbul, Turkey; Email: akincitc@itu.edu.tr

Serhat Seker: Department of Electrical Engineering, Istanbul Technical University, Maslak, Istanbul, Turkey

Erkan Dursun: Department of Electrical & Electronics Eng., Marmara University, Faculty of Technology, Istanbul, Turkey

Osman Kilic: Department of Electrical & Electronics Engineering, Marmara University, Istanbul, Turkey

Table 1: Subsystems of the hydrogen fuel cell system and their components.

Subsystems	Auxiliary subsystems of the hydrogen fuel cell	
		Components
I. Air supply and control subsystem	Air compressor and expander; Supply manifold; Cathode side of the fuel cell stack; Return manifold and back pressure control valve.	
II. Fuel supply and control subsystem	High-pressure fuel tank; Pressure regulator; Supply manifold; Anode side of the fuel cell stack and purge control valve.	
III. Water management subsystem	Air/fuel humidifiers or vapor injector and vapor condenser.	
IV. Thermal management subsystem	Cooling loop for the stack and temperature control for humidifiers and a radiator.	

Mathematical modelling is necessary for improvements in fuel cell performance and operation to get better design and optimization. In this sense, there are many published models for PEM fuel cells in the literature. There are several approaches to fuel cell modelling related to:

1. Equations or characteristics of fuel cell models;
2. Number of dimensions for the models (one or more);
3. Dynamic or Steady-State;
4. Anode/Cathode kinetics and phase (Gas, liquid or their combinations);
5. Mass transport (such as electrolyte);
6. Membrane Swelling (Empirical or Thermodynamic models);
7. Energy Balance.

The main stages of the model-building process are:

- Model selection,
- Model fitting,
- Model validation.

These steps are iteratively used until an appropriate model for the data has been obtained [14].

In this study, a linear transfer function defined between the DC electricity and hydrogen flow as a simplified model is suggested. This method is a rather different approach from the given examples above because it is connected with the signal-based approach. In this manner, this different view-point to the fuel cell modelling may create some new possibilities like the frequency response characteristic and stability of the cell.

The organization of this study is based on “Data Acquisition”; “Spectral Analysis” and “Simplified Transfer Function Approach” as follows.

2 Measurement system and data acquisition

A hydrogen fuel cell system involves the following four auxiliary subsystems like.

- Air supply and control subsystem,
- Fuel supply and control subsystem,
- Water management,
- Thermal management subsystem.

These subsystems include some basic components as shown in Table 1.

These four subsystems have a large effect on the performance of the fuel cell stack as well as efficiency [25]. In the fuel cell stack, 10 single cells are connected in series. The current is tapped through the current collectors at the two endplates. And also, a measurement system connected with the fuel cell system can be represented as shown in Figure 1.

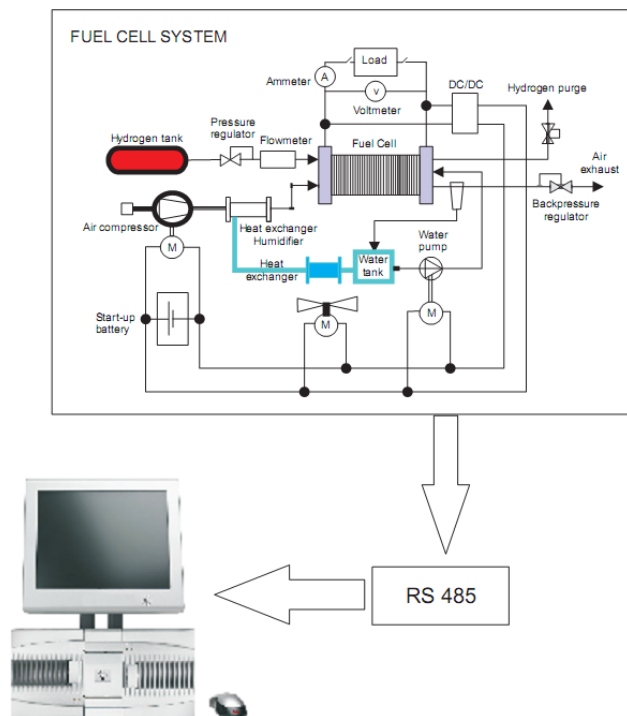
The computer monitors all system parameters of the fuel cell system through the RS485 data connections. Also, the fuel cell parameters are demonstrated in Table 2. Using this measurement and data acquisition system, the data such as hydrogen flow, temperature, pressure and power as well as cell current and voltage are collected and processed.

3 Mathematical methods

Regarding the mathematical methods, the approaches based on Fourier transform are considered as follows.

Table 2: Fuel cell parameters

	Parameter of Fuel Cell
Rated power output	40 W
Maximum power output	Approx. 50 W
Open circuit voltage	Approx. 9 V
Current at rated power	8 A
Voltage at rated power	5 V
Maximum current	10 A
Hydrogen consumption during rated output	Approx. 580 NmL/min
Hydrogen nominal pressure	0.6±0.1 bar gauge
Maximum permissible hydrogen pressure	0.4...0.8 bar gauge
Maximum permissible cell temperature	Operation 50 C Starting 45 C
Supply voltage	12 VDC
Power consumption	No-load operation 5.2 W at 10 A load current 6.4 W
Hydrogen connection	Swagelok @quick coupler type QM2-S
Ambient operating temperature	+5...+35 C
Dimensions	400×297×200 mm
Weight	3.5 kg

**Figure 1:** Measurement System.

3.1 Power Spectral Density (PSD)

A common approach to get information about the frequency features of a random signal is to transform the signal to the frequency domain by computing the Discrete

Fourier Transform (DFT). For a block of data of length N samples, the transform at frequency $m\Delta f$ is given by,

$$X(m\Delta f) = \sum_{k=0}^{N-1} x(k\Delta t) \exp[-j2\pi km/N] \quad (1)$$

Here, Δf is the frequency resolution and Δt is the data-sampling interval. The auto-power spectral density (APSD) of $x(t)$ is estimated as

$$S_{xx}(f) = \frac{1}{N} |X(m\Delta f)|^2, f = m\Delta f \quad (2)$$

The cross power spectral density (CPSD) between $x(t)$ and $y(t)$ is estimated in a similar way. The statistical accuracy of the prediction in Equation (2) increases as the number of data points or the number of blocks of data increases [19, 23].

3.2 Short-Time Fourier Transform

The Short-Time Fourier Transform (STFT) introduced by Dennis Gabor 1946 has been useful in rendering the time localization of frequency components of signals. The STFT spectrum is gained by windowing the signal via a fixed dimension window. The signal can be thought almost stationary in this window. The window dimension fixed both time and frequency resolutions. So as to define the STFT, we can take a signal $x(t)$ with the assumption that it is

stationary when it is windowed through a fixed dimension window $g(t)$, centred at time location τ . The Fourier transform of the windowed signal yields the STFT [19, 23].

$$STFT \{x(t)\} \equiv X(\tau, f) = \int_{-\infty}^{+\infty} x(t)g(t - \tau) \exp[-j2\pi ft] dt \quad (3)$$

The equation maps the signal into a two-dimensional function in the time-frequency (t, f) plane. The analysis depends on the chosen window $g(t)$. Once the window $g(t)$ has been selected, the STFT resolution is fixed over the entire time-frequency plane. In a discrete case, it becomes,

$$STFT \{x(n)\} \equiv X(m, f) = \sum_{n=-\infty}^{+\infty} x(n)g(n - m) e^{-jwn} \quad (4)$$

The magnitude squared of the STFT yields the “spectrogram” of the function.

$$Spectrogram \{x(t)\} \equiv |X(\tau, f)|^2 \quad (5)$$

4 Application to data

In this study, the collected data are provided using the HY-Expert Fuel Cell System hardware as indicated in Figure 1. In this manner, the voltage and current variations can be shown in Figure 2.

As seen in Figure 2, there are periodically some jumping on the current and voltage variations. These are connected with the over peaks in the hydrogen flow. This property of the hydrogen flow can be easily observed from Figure 3.

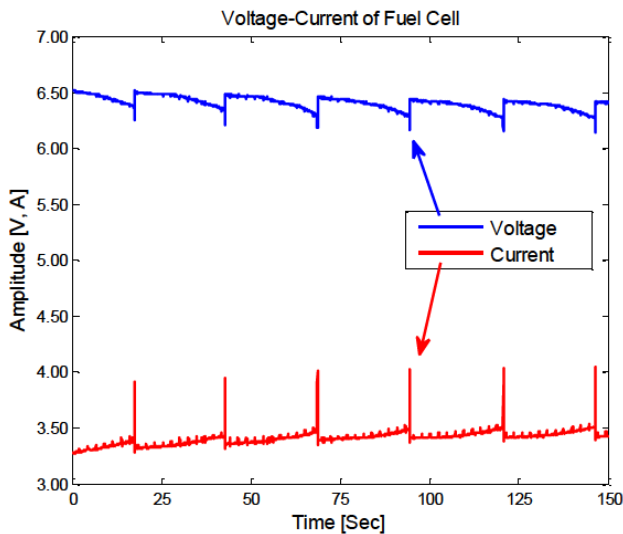


Figure 2: Current [A] and Voltage [V] variations of the Fuel Cell System.

With respect to the ascertainment of frequency characteristics of the fuel cell measurements, the Power Spectral Density (PSD) calculations, as shown in section 3, can be assessed for the voltage, current and hydrogen flow variations. In this sense, spectral changes related to the system can be described between the 0 and 15 Hz as seen in Figures 3 and 4. However, noise like effect can be observed after the 15 Hz for hydrogen flow. In this manner, some frequency components of the spectra, which are greater than the 15 Hz, can be interpreted as measurement noise.

This is the characteristic of hydrogen feeding pump as shown in Figure 3. As shown in Figure 6, normal variation is between 0-15 Hz which is low-frequency region of the spectrum, but after the frequency of 30 Hz it becomes

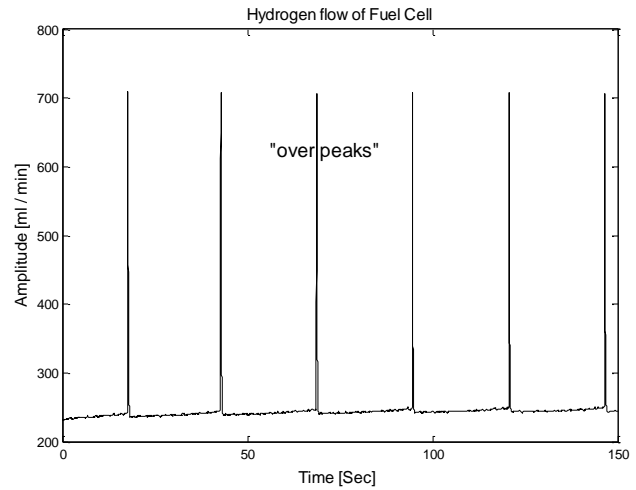


Figure 3: Measurement of the Hydrogen flow.

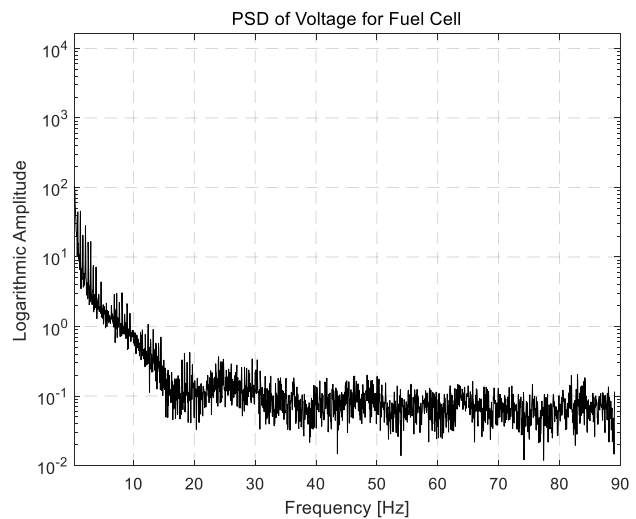


Figure 4: Semi-Logarithmic Power Spectral Density (PSD) variation for voltage measurement.

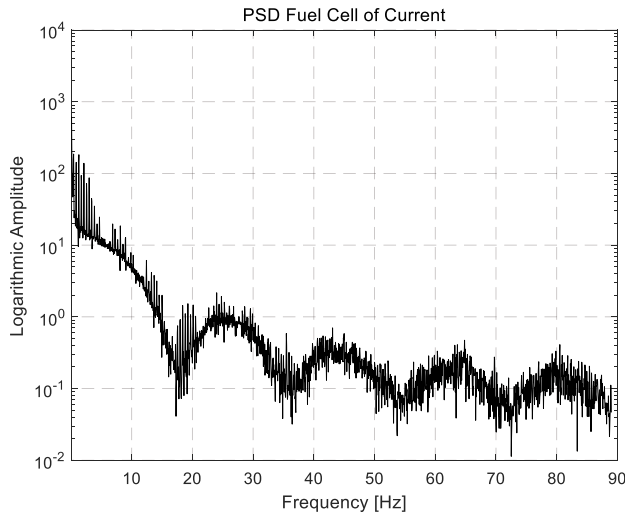


Figure 5: Semi-Logarithmic Power Spectral Density (PSD) variation for current measurement.

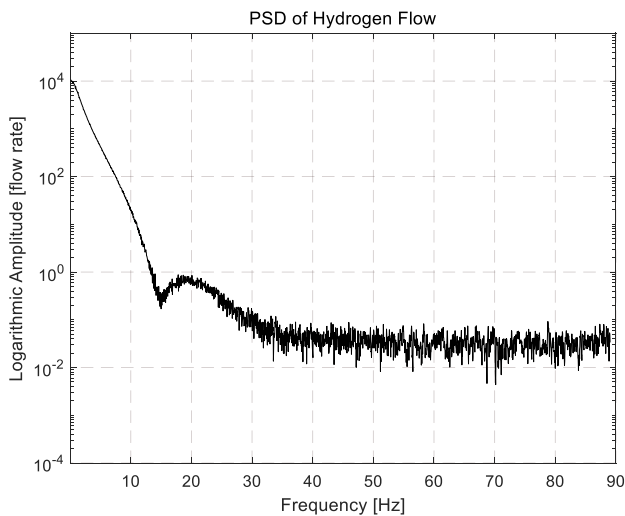


Figure 6: Semi-Logarithmic Power Spectral Density (PSD) variation for hydrogen flow measurement.

white noise (it is constant) and it doesn't include any physical information.

Semi-Logarithmic Power Spectral Density (PSD) variations for hydrogen flow measurement is provided in Figure 6, where the total frequency range is between 0-90 Hz and its spectral band can be classified as below;

- i) 0-15 Hz: System response
- ii) 15-30 Hz: Transition range from system response to the White noise region.
- iii) 30-40 Hz: mixing with the hydrogen flow and process noise.
- iv) This is the pure white noise region.

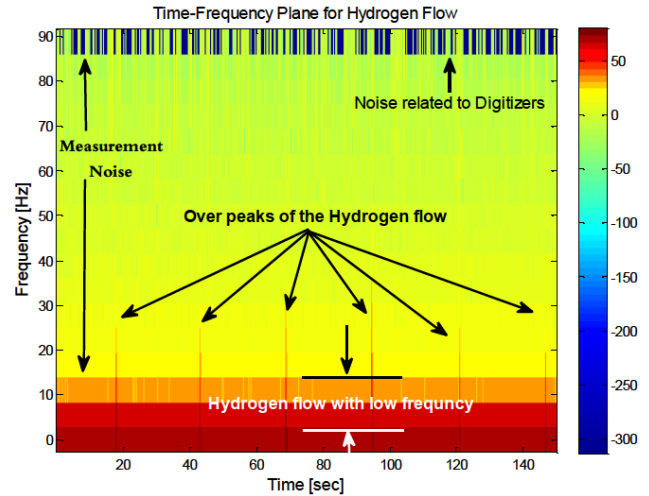


Figure 7: Spectrogram of the hydrogen flow.

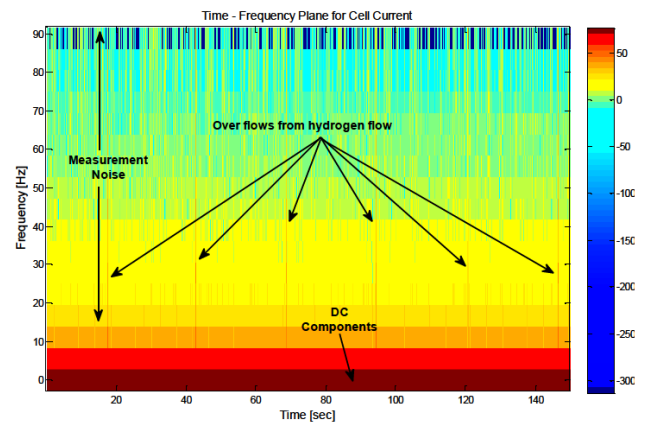


Figure 8: Spectrogram of the cell current.

It means that the part of (0-15 Hz) is an informative band and it shows the information that comes from the interaction between the hydrogen flow and system (fuel-cell). Hence after roughly 30 Hz this interaction is increasing with process noise, and then the total noise goes to the white noise between 40 and 90 Hz.

If there is no fuel cell, then it cannot be said the interaction between the hydrogen flow and process-noise in the fuel cell. Hence any information cannot be extracted.

Moreover, for more detailed spectral analysis, if it is considered the spectrograms for each measurement like hydrogen flow and current variations. They are shown by Figure 7 and Figure 8.

As seen in Figure 7, the over peaks in the hydrogen flows appear on the time-frequency plane. The average frequency value of these peaks at around the 30 Hz and measurement noise begins after the 15 Hz. Frequency region between the 15 and 90 can be accounted for the noise region arising from the measurement circuits and digitizers.

Considering Figure 8, the cell current as DC electricity can be described at around 0 Hz overall time. And also, there are additional spectral components between the 0-15 Hz as well as the DC component. These frequency components can be easily identified from the current variation in the time-domain. Here, these variations are seen as lobes. Furthermore, the noise parts that come from the digitizers are observed between 85 and 90 Hz.

5 Simplified transfer function of the fuel cell

During this study, considered data are related to the hydrogen flow and current measurements. In this sense, spectral analysis of these data can be used to extract the useful information regarding the frequency response of the fuel cell. For this aim, the frequency response or transfer function of the fuel cell can be described between the cell current and hydrogen flow measurements under the assumption of linearity. So, this situation can be shown in a most simplified manner by the following block-diagram.

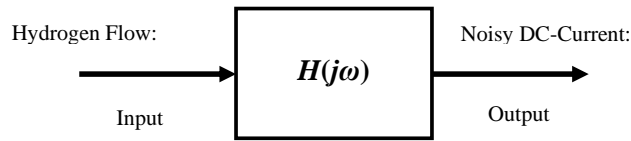


Figure 9: Linear transfer function model of the fuel cell.

Where the transfer function can be given with a ratio defined between the input and output pair in the frequency domain.

$$H(j\omega) = \frac{Y(j\omega)}{X(j\omega)} \quad (6)$$

Here X and Y are the Fourier transforms of the input and output of the fuel cell respectively. However, the transfer function $H(j\omega)$ is a complex-valued function, accordingly, its amplitude is believed to show the magnitude variation. For this case, the magnitude variation can be defined as,

$$|H(j\omega)| = \frac{|Y(j\omega)|}{|X(j\omega)|} \hat{=} \frac{PSD \{Noisy DC - Current\}}{PSD \{Hydrogen Flow\}} \quad (7)$$

Here symbol $|\cdot|$ and $PSD \{.\}$ indicate the magnitude of a complex-valued function and Power Spectral Density respectively. Hence the plot of the Equation (7) can be shown by Figure 10.

Where, the magnitude variation of the transfer function reflects physical, chemical and measurement related

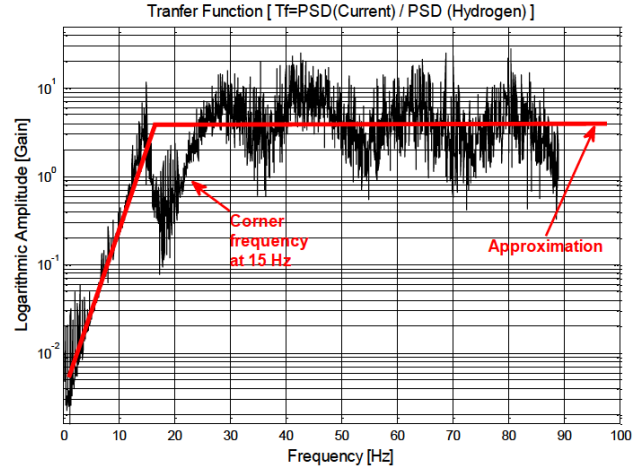


Figure 10: Magnitude variation of the fuel cell transfer function.

effects of the fuel cell in the frequency domain. These effects are very suitable with the individual properties of each data. All detailed results about this matter are given in the section of concluding remarks as follows.

6 Concluding remarks

This study is based upon spectral analysis of the data which are collected from the fuel cell in a laboratory medium. For this purpose, the related data like current, voltage and hydrogen flow are examined for both of the amplitude-frequency and time-frequency planes as well as their time-domain variations. Also, joint information about the spectral behaviour of the fuel cell is extracted under the linear transfer function approach. In this sense, the transfer function model of the fuel cell is defined by Equation (7). The amplitude variation of the transfer function is used for noise identification on the overall frequency range.

Here, the most interesting viewpoint is to study the various noise effects of the fuel cell although its output is in the DC character. However, some frequency components on the DC (Direct current) are considered as a noise part and it is classified under several types.

Consequently, the magnitude variation of the fuel cell transfer function looks like a high pass filter characteristic as seen in Figure 10. If so, its corner frequency becomes at around 15 Hz approximately. Also, spectral components between 0-15 Hz as seen in Figures 7 and 8 can be interpreted as the process noise of the fuel cell. Between 0-15 Hz it is the interaction between H_2 flow and physical structure, for this reason, it carries some information about the

physical system. So, it is accepted as process noise with small fluctuations.

Finally, the spectral range for this application can be categorized under three regions, these are listed below:

1. Process noise between 0-15 Hz.
2. Measurement noise between 15-90 Hz.
3. Digitization affects around 90 Hz.

Where, the process noise to have occurred at very small frequencies ~0-8 Hz (<15 Hz) can be interpreted as some effects which come from the various physical and chemical interactions in the fuel cell. These effects can be represented by fluctuation appeared as results of the membrane swelling, proton exchange and anode/cathode kinetics.

As future work, this transfer function approach can be expanded to the stability studies on the fuel cells.

Acknowledgement: We are grateful to authorized persons of UNIDO-ICHET (United Nations Industrial Development Organization - International Centre for Hydrogen Energy Technologies) for their help in providing the data used in this study.

References

- [1] Araya S.S., Zhou F., Sahlin S.L., Thomas S., Jeppesen C., Kőr S.K., Fault characterization of a proton exchange membrane fuel cell stack, *Energies*, MDPI, 2019, 12(152), 1-17.
- [2] Astafev E., Frequency characteristics of hydrogen-air fuel cell electrochemical noise, *Fuel Cell*, Wiley-Vch Verlag, 2018, 18(6), 755-762.
- [3] Barbir F., *PEM fuel cells: theory and practice*, 2005, Elsevier Academic Press, London, UK.
- [4] EG & G Technic Services, *Fuel Cell Hand Book*, 7th Ed., 2004 <https://netl.doe.gov/sites/default/files/netl-file/FCHandbook7.pdf>
- [5] Funk J.E., Thermochemical hydrogen production: past and present, *Int. J. Hydr. Energy*, 2001, 26(3), 185-190.
- [6] *Hydrogen & Fuel Cell*, Review of national R&D program, 2004, OECD/IEA.
- [7] Instructor Training System - Fuel cell store, Experiments guide and components description for the Hy-Expert™, 5th Edition, 2011, <http://fuelcellstore.com/manuals/693-fuel-cell-trainer-experiment-guide.pdf>
- [8] Kaytakoğlu S., Akyalçın L., Optimization of parametric performance of a PEMFC. *Int. J. Hydr. Energy*, 2007, 32(17), 4418-4423.
- [9] Knights S.K., Colbow K., St-Pierre J., Wilkinson D., (2004), Aging mechanisms and lifetime of PEFC and DMFC, *J. Power Sources*, 2004, 127(1-2), 127-134.
- [10] Larminie J., Dicks A., *Fuel cell systems explained*, Second ed., 2003, Wiley and Sons, England.
- [11] Luo Z., Li D., Tang H., Pan M., Ruan R., Degradation behaviour of membrane-electrode-assembly materials in 10-cell PEMFC stack, *Int. J. Hydr. Energy*, 2006, 31(13), 1831-1837.
- [12] Miede A., Steffena F., Luschinetza T., Jakubith S., Freitag M., Real time water detection for adaptive control strategy in pemfc-systems, *Energy Procedia*, 2012, 29, 431-437.
- [13] Schimmel H.G., *Towards a hydrogen-driven society?*, 2004, DUP Science, Netherlands.
- [14] Spiegel C., *PEM fuel cell modeling and simulation using MATLAB*, 2018, Elsevier Inc.
- [15] Waller L., Kim J., Shao-Horn Y., Barbastathis G., Interferometric tomography of fuel cells for monitoring membrane water content, *Optics*, 2009, 17(17), 14806-14816.
- [16] Le A.D., Zhou B., A Numerical Investigation on multi-phase transport phenomena in a proton exchange membrane fuel cell stack, *J. Power Sources*, 2010, 195(16), 5278-5291.
- [17] LaConti A., Hamilton M., McDonald R., *Handbook of Fuel Cells-Fundamentals. Technology and Applications*, 2003, Wiley.
- [18] St-Pierre J., PEMFC in Situ liquid water content monitoring status, *J. Electrochem. Soc.*, 2007, 154(7), B724-B731.
- [19] Taskin S., Seker S., Karahan M., Akinci T.C., Spectral analysis for current and temperature measurements in power cables, *Electric Power Compon. Syst.*, 2009, 37(4), 415-426.
- [20] Waller L., Kim J., Shao-Horn Y., Barbastathis G., Interferometric tomography of fuel cells for monitoring membrane water content, *Optics Express*, 2009, 17(17), 14806-14816.
- [21] Wan Z., Chang H., Shu S., Wang Y., Tang H., A review on cold start of proton exchange membrane fuel cells, *Energies*, 2014, 7(5), 3179-3203.
- [22] Witkowska A., Principi E., Di Cicco A., Marassi R., Advanced XAS analysis for investigating fuel cell electrocatalysts, XAFS13: 13th Int. Conf. (9-14 July 2006, Stanford, California), CA, USA.
- [23] Vaseghi S.V., *Advanced signal processing and digital noise reduction*, 1996, John Wiley & Sons Inc.
- [24] Veziroğlu T.N., Barbir F., *Emerging Technology Series - Hydrogen Energy Technologies*, 1998, UNIDO, Vienna.
- [25] Zhao H., Burke A.F., Optimization of fuel cell system operating conditions for fuel cell vehicles, *J. Power Sources*, 2009, 186(2), 408-416.